

Stimulation of PHB Production in *Chlorella vulgaris* for Use as Bioplastic

Hager M. Abd El-Latif^{1*}, Wafaa S. Abou El-Kheir¹, Afaf H. Ali¹, Rawia F. Sadeck², S.A. Abdelkader¹

¹Department of Botany, Faculty of Women for Arts, Sciences and Education, Ain Shams University, Egypt

²Researcher in department of Drug Radiation Research, National Center for Radiation Research and Technology (NCRRT), Atomic Energy Authority, Egypt (AEA), Cairo, Egypt

*Corresponding Author: hajar@women.asu.edu.eg

ARTICLE INFO

Article History:

Received: May 22, 2025

Accepted: July 18, 2025

Online: July 27, 2025

Keywords:

Chlorella,
Bioplastic,
PHB,
Degradation,
FTIR

ABSTRACT

Polyhydroxybutyrate (PHB) is a biodegradable polymer that naturally stores carbon and is produced by a variety of microorganisms, including certain algal species. It presents a viable alternative to conventional plastics due to its ability to degrade without leaving toxic residues. In this study, *Chlorella vulgaris* was used to optimize PHB production under varying light intensities and sodium acetate supplementation. The highest PHB yield was observed in the PHB-T3 treatment (1364µg/ g), compared to 850µg/ g in PHB-T1, indicating that the addition of sodium acetate significantly enhanced PHB synthesis. Following PHB extraction, three types of bioplastic films were produced: two from PHB extracts (PHB-T1 and PHB-T3) and one directly from *C. vulgaris* biomass. Among these, the *C. vulgaris*-based film exhibited superior physical characteristics—it was thicker, structurally more uniform, and free from surface cracks when compared to the PHB-derived films. All films demonstrated high solvent solubility at 60°C, suggesting enhanced thermal performance. Moisture absorption tests revealed that the *C. vulgaris* film had the highest absorption rate (25%), followed by PHB-T3 (15%) and PHB-T1 (10%), suggesting potential applications where water interaction is beneficial. Mechanical testing further highlighted the advantages of the *C. vulgaris* film, which exhibited greater tensile strength and elongation, making it more suitable for applications requiring both flexibility and durability. Biodegradability tests conducted in clay soil showed rapid degradation for all film types, confirming their environmental compatibility. Overall, the findings demonstrate the potential of PHB and *C. vulgaris*-based films in the development of sustainable materials. Each film type offers distinct advantages depending on the specific application, with *C. vulgaris*-derived films excelling in mechanical integrity and moisture responsiveness.

INTRODUCTION

Plastics derived from fossil fuels offer several advantages, including long shelf life and high resistance to environmental degradation (Chong *et al.*, 2022). However, the global surge in the demand for synthetic plastics has led to severe environmental

consequences, particularly in marine ecosystems. In response, the global market has increasingly shifted toward the use of bioplastics—sustainable and environmentally friendly alternatives to conventional plastics (**Formela *et al.*, 2022**). The bioplastics market is projected to grow rapidly in the coming years, driven by rising public awareness about environmental protection, stricter regulations on waste management, and the emphasis on sustainable use of natural resources (**Mohamed *et al.*, 2024**).

Among the most promising resources for bioplastic production are microalgae due to their remarkable adaptability to various environmental conditions, high productivity, and efficient water use. Unlike terrestrial crops, microalgae do not compete with food production and can thrive on nutrient-rich wastewater, making them an ideal raw material for sustainable bioplastic production (**Kaparapu, 2018**). Numerous reviews have investigated microalgae-based bioplastics (**Zhang *et al.*, 2019**; **Onen Cinar *et al.*, 2020**; **Kartik *et al.*, 2021**; **Madadi *et al.*, 2021**; **Dang *et al.*, 2022**; **Park & Lee, 2022**; **Arora *et al.*, 2023**), focusing on naturally occurring algal polymers such as polyhydroxyalkanoates (PHAs), polysaccharides, and proteins, as well as blends of microalgal biomass with other polymers.

Microalgae can be used directly in bioplastic production as whole biomass or indirectly by extracting specific biopolymers like polyhydroxybutyrate (PHB). PHB, a type of PHA, is composed mainly of 3-hydroxybutyrate (3HB) and, to a lesser extent, 3-hydroxyvalerate (3HV) and 3-hydroxyhexanoate (3HH). It exists in an amorphous form inside algal cells but crystallizes upon extraction (**Nanda & Bharadwaja, 2022**). In recent years, PHB from microalgae has attracted attention as a cost-effective and sustainable alternative to petrochemical plastics (**Costa *et al.*, 2018**).

One of the most promising algal species for this purpose is *Chlorella vulgaris*, a green microalga characterized by its small cell size, rapid growth rate, and high protein (50.20%) and carbohydrate (41.92%) content (**Zainan *et al.*, 2018**). According to **Sabathini *et al.* (2018)**, *Chlorella*-based films exhibit strong tensile strength (up to 35.1 kg/cm²) and improved surface properties when blended with polyvinyl alcohol (PVA) using ultrasonic homogenization. Additionally, **Robert and Iyer (2018)** successfully used *C. vulgaris* to optimize PHB production for bioplastic synthesis.

Numerous studies have explored different strategies to enhance PHB yield and modify its properties through optimization of culture conditions (e.g., pH, temperature, nutrient levels, and carbon source), as well as various extraction methods—chemical (e.g., solvent-based), physical (e.g., bead milling, ultrasonication), and biological (e.g., enzymatic digestion) (**Costa *et al.*, 2018**; **García *et al.*, 2020**; **Hassan *et al.*, 2024**).

This study aimed to enhance the production of PHB from *Chlorella vulgaris* under optimized culture conditions and to develop bioplastic films from both the extracted PHB and whole algal biomass. The ultimate goal is to offer an environmentally sustainable alternative to conventional plastics, thereby reducing ecological risks and contributing to the development of biodegradable materials.

MATERIALS AND METHODS

1. Cultivation of microalgae

Chlorella vulgaris was obtained from the National Institute of Oceanography and Fisheries, El-Kanater El-Khiria, Qalyubia, Egypt. Cultivation was conducted using BG-11 medium, which was sterilized by autoclaving for 20 minutes prior to inoculation (Stanier *et al.*, 1971).

2. Optimization of PHB production

2.1 Experimental treatments

C. vulgaris was grown under four different conditions to determine optimal growth for PHB production. Treatments were evaluated based on chlorophyll *a* content and optical density (OD), indicators of algal biomass. Cultures were incubated at $25 \pm 2^{\circ}\text{C}$, pH 7.5, under sterile conditions for 30 days. Each treatment was replicated. The treatments included:

- **T1 (Control):** Cultures exposed to natural sunlight through a window with a photoperiod of 16/8 h (light/dark).
- **T2 (Artificial Light):** Cultures exposed to artificial lighting using three white LEDs (20W, 2000 lumens) placed 40cm above the bench (Abou-El-Souod *et al.*, 2016).
- **T3 (Sodium Acetate + Natural Light):** Cultures supplemented with 1g/ L sodium acetate and exposed to natural sunlight (Robert & Iyer, 2018).
- **T4 (Sodium Acetate + Artificial Light):** Cultures supplemented with 1g/ L sodium acetate and exposed to artificial lighting using white LEDs (20W, 2000 lumens) (Maheswari & Ahilandeswari, 2011).

2.2 Growth parameters

Growth was monitored by measuring chlorophyll *a* and optical density (OD) every two days over 30 days:

- Chlorophyll *a* was extracted and quantified using absorbance at 644 and 663nm. The concentration was calculated using the equation of Metzner *et al.* (1965):

$$\text{Chlorophyll (a)} = 10.3 \text{ OD } 663 - 0.918 \text{ OD } 644 \text{ } \mu\text{g/ml}$$

- Optical Density (OD) was measured at 680nm using a spectrophotometer (El-Sheekh *et al.*, 2021).

3. Large-scale cultivation, harvesting, and drying

Based on the results, T3 was identified as the optimal condition for large-scale cultivation. Cultures for T1 and T3 were scaled up in 20L transparent polyethylene bottles containing BG-11 medium. Cultures were maintained at $25 \pm 2^\circ\text{C}$, pH 7.5, and continuously aerated for 26 days (T1) and 14 days (T3). Harvesting was carried out via centrifugation at 4000 rpm for 20 minutes, followed by rinsing with distilled water, air-drying, oven-drying, and grinding into fine powder.

4. PHB extraction

PHB was extracted from the dried biomass of T1 and T3 cultures following the method of Robert and Iyer (2018). Biomass was centrifuged at 2000 rpm for 20 minutes, and PHB concentration was quantified using a standard curve. Extracts were labeled PHB-T1 and PHB-T3.

5. FTIR characterization of PHB

Fourier-transform infrared spectroscopy (FTIR) was performed at the National Center for Radiation Research and Technology (NCRRT), Atomic Energy Authority (AEA), Egypt. The PHB polymers from PHB-T1 and PHB-T3 were analyzed with a resolution of 4cm^{-1} over the wavelength range $400\text{--}4000\text{cm}^{-1}$.

6. Bioplastic film formation

6.1 From *C. vulgaris* Biomass

Bioplastic films were prepared using *C. vulgaris* biomass following Sabathini *et al.* (2018). The biomass was mixed with distilled water, poured into silicone molds, and air-dried for 24 hours at room temperature before being peeled off to obtain dried films.

6.2 From PHB extracts

Bioplastics from PHB-T1 and PHB-T3 were prepared following the method of Wu *et al.* (2009). The extracted PHBs were processed and cast into bioplastic films.

7. Bioplastic characterization

7.1 *Physical properties*

7.1.1 Color and texture

Visual inspection was used to assess the color uniformity and texture consistency of the films.

7.1.2 Solubility in solvents

Film solubility was tested by placing 0.3g of each bioplastic film in test tubes containing 3mL of solvents (acetone, ethanol, and chloroform). Samples were incubated under two conditions:

- Room temperature ($25 \pm 2^{\circ}\text{C}$)
- Heated to 60°C . Solubility was assessed after 1 hour (**Tun & Mar, 2020**).

7.1.3 Moisture absorption

Dried bioplastic samples were weighed (W_1) after storage in a desiccator, then exposed to ambient air for 24 hours and reweighed (W_2). Moisture absorption was calculated as a percentage increase in weight (**Tun & Mar, 2020**). The moisture absorption percentage was determined by using the formula:

$$\text{Moisture absorption (\%)} = \frac{(W_2 - W_1)}{W_1} \times 100$$

7.2. *Mechanical properties*

Tensile strength (TS) and elongation at break (EAB %) were analyzed using Tinius Olsen H10KS and performed at NCRRT, AEA, Egypt.

7.3. *Morphological properties*

The morphological characteristics of the bioplastic films surfaces were determined using scanning electron microscopy (SEM) at the NCRRT, AEA, Egypt, at 500x magnification.

7.4. *Chemical properties*

7.4.1. Fourier transform infrared spectroscopy (FTIR)

FTIR analysis was performed with the same equipment and procedures mentioned above.

7.4.2. X-Ray diffraction (XRD)

XRD analysis was also performed at NCRRT, AEA, Egypt using X-ray diffraction with a scanning range of 100 - 90° at a scanning speed of 8.0000 (°/min) with a sampling pitch 0.02.

7.5. Biological properties

7.5.1. Biodegradation by soil

Fixed weights from all bioplastic films were buried under the clay and sandy soil surface for 30 days and then the weights were recorded again (Nguyen *et al.*, 2016). Then the weight loss percentage was calculated using the following equation:

$$\text{WL}\% = \frac{\text{initial wt.of the film} - \text{wt.of the film after degradation}}{\text{initial wt.of the film}} \times 100$$

7.5.2. Biodegradation by water

According to Naesa *et al.* (2019), a constant weight of all bioplastic films is placed in different water media (distilled water, acidic water and alkaline water). Degradation measured after 7 and 14 days using the following equation:

$$\text{WL}\% = \frac{\text{initial wt.of the film} - \text{wt.of the film after degradation}}{\text{initial wt.of the film}} \times 100$$

8. Statistical analysis

All data were statistically analyzed using one-way analysis of variance ANOVA. Significant differences among variable treatments were identified using Duncan's Multiple Range Test (DMRT) conducted with SPSS software (version 16) (SPSS, 2012).

RESULTS

Estimation of photosynthetic pigment (chlorophyll *a*) and optical density (OD) as growth parameters

The results presented in Table (1) show significant differences ($P < 0.001$) in chlorophyll *a* content across the four treatments. The highest chlorophyll *a* concentration was recorded in T1 ($43.95 \pm 1.40 \mu\text{g/mL}$) after 28 days, corresponding to a daily accumulation rate of $1.57 \mu\text{g/mL/day}$. This was followed by T2, which reached $23.54 \pm 1.70 \mu\text{g/mL}$ after 22 days ($1.07 \mu\text{g/mL/day}$). T3 reached a maximum of $19.94 \pm 0.50 \mu\text{g/mL}$ after only 13 days, with a comparable accumulation rate of $1.53 \mu\text{g/mL/day}$, indicating a faster growth cycle. The lowest chlorophyll *a* content was observed in T4, with $16.13 \pm 0.35 \mu\text{g/mL}$ after 19 days, corresponding to $0.85 \mu\text{g/mL/day}$.

These findings indicate that while T1 achieved the highest overall chlorophyll *a* concentration, T3 offered a favorable balance between growth rate and productivity over a shorter cultivation period.

Table 1. The chlorophyll-a content ($\mu\text{g/ml}$) of *C. vulgaris* at T1, T2, T3 and T4 treatments

Treatments Day's number	Chlorophyll-a ($\mu\text{g/ml}$)			
	T1 (control)	T2	T3	T4
0	0.65 ± 0.10^h	0.65 ± 0.10^h	0.65 ± 0.10^h	0.65 ± 0.10^h
2	2.36 ± 0.50^f	1.87 ± 1.60^h	$2.34 \pm 1.00^{f,g,h}$	$1.57 \pm 0.60^{g,h}$
4	3.60 ± 0.40^f	2.06 ± 1.00^h	$5.60 \pm 1.00^{e,f,g}$	$2.23 \pm 0.23^{f,g}$
6	$5.35 \pm 0.90^{e,f}$	3.65 ± 0.50^h	$8.39 \pm 0.90^{b,c,d}$	5.87 ± 2.00^e
8	7.01 ± 2.00^e	6.05 ± 0.50^g	$11.16 \pm 1.50^{b,c}$	$7.26 \pm 0.20^{d,e}$
10	7.06 ± 0.60^e	$9.11 \pm 0.70^{e,f}$	$13.02 \pm 1.20^{b,c}$	10.85 ± 0.80^c
12	10.61 ± 1.20^d	$9.44 \pm 1.50^{d,e,f}$	$15.08 \pm 0.45^{b,c}$	13.18 ± 0.45^b
14	13.89 ± 2.50^c	$9.93 \pm 0.90^{d,e,f}$	19.94 ± 0.50^a	10.68 ± 1.40^c
16	14.64 ± 1.50^c	$11.03 \pm 1.00^{d,e}$	9.61 ± 2.00^b	12.89 ± 0.80^c
18	15.84 ± 0.80^c	11.21 ± 0.90^d	$8.94 \pm 1.90^{b,c}$	15.08 ± 0.45^a
20	21.19 ± 0.19^b	15.83 ± 1.30^c	$7.12 \pm 1.80^{c,d,e}$	16.13 ± 0.35^a
22	21.28 ± 1.40^b	20.22 ± 0.70^b	$4.73 \pm 1.60^{f,g}$	8.64 ± 0.60^d
24	20.76 ± 0.70^b	23.54 ± 1.70^a	$4.5 \pm 1.50^{f,g,h}$	6.46 ± 0.55^e
26	43.95 ± 1.40^a	15.83 ± 0.50^c	$3.22 \pm 0.45^{g,h}$	3.22 ± 1.20^f
28	15.86 ± 2.00^c	8.85 ± 1.00^f	2.37 ± 0.29	$2.04 \pm 0.70^{f,g,h}$
30	13.21 ± 1.50^c	6.75 ± 1.50^c	2.29 ± 0.29^h	1.22 ± 0.60^c
F value	190.95***	110.86***	33.85***	110.58***

Values are presented as mean \pm standard deviation. Significant at $P < 0.001$. The values of identical letters within the same column are not significantly different based on Duncan's Multiple Range Test.

The optical density of *C. vulgaris*, as shown in Table (2), reached its highest value of 1.93 ± 1.20 at T1 on day 26 followed by T2 (1.72 ± 0.78) on day 24. T3 recorded an OD of 1.55 ± 0.88 on day 14, while T4 reached the value of 1.51 ± 0.65 on day 20. The results suggest that T3 is the best condition, as it achieved the highest algal growth rate within the shortest time. Therefore, T3 was cultivated on a large scale compared to the control (T1).

Table 2. Optical density (OD) of *C. vulgaris* at T1, T2, T3 and T4 treatments

Treatments Day's number	Optical density (OD)			
	T1 (control)	T2	T3	T4
0	0.04 ± 0.02	0.04 ± 0.02	0.04 ± 0.02	0.04 ± 0.02
2	0.09 ± 0.03^{bc}	0.08 ± 0.01^c	0.11 ± 0.16^{cd}	0.09 ± 0.13^{cd}
4	0.10 ± 0.05^c	0.13 ± 0.05^c	0.22 ± 0.15^{cd}	0.14 ± 0.05^{cd}
6	0.13 ± 0.11^{bc}	0.14 ± 0.08^c	0.31 ± 0.15^{cd}	0.22 ± 0.12^{bcd}
8	0.22 ± 0.15^{bc}	0.21 ± 0.02^{bc}	0.56 ± 0.28^{bcd}	0.24 ± 0.15^{bcd}
10	0.49 ± 0.25^{abc}	0.39 ± 0.15^{abc}	0.77 ± 0.40^{abcd}	0.70 ± 0.58^{abcd}
12	0.56 ± 0.45^{abc}	0.98 ± 0.54^{abc}	1.29 ± 0.70^{ab}	0.87 ± 0.55^{abc}

14	0.73 ± 0.58^{abc}	1.00 ± 0.40^{abc}	1.55 ± 0.88^a	1.10 ± 0.50^{abc}
16	0.75 ± 0.15^{abc}	1.24 ± 0.60^{abc}	1.35 ± 0.88^{ab}	1.16 ± 0.79^{abc}
18	1.04 ± 0.95^{abc}	1.32 ± 1.10^{abc}	1.28 ± 0.65^{abc}	1.32 ± 0.80^a
20	1.05 ± 0.75^{abc}	1.49 ± 0.89^{ab}	1.11 ± 0.45^{abc}	1.51 ± 0.65^a
22	1.22 ± 0.89^{abc}	1.62 ± 1.20^a	0.97 ± 0.46^{abcd}	1.49 ± 0.76^a
24	1.32 ± 1.10^{ab}	1.72 ± 0.78^a	0.95 ± 0.22^{bcd}	1.38 ± 0.44^a
26	1.93 ± 1.20^a	1.61 ± 1.20^a	0.76 ± 0.33^{abcd}	1.19 ± 0.54^{ab}
28	1.01 ± 0.95^{ab}	1.23 ± 0.57^{abc}	0.56 ± 0.22^{bcd}	0.98 ± 0.25^{abcd}
30	0.99 ± 0.32^{abc}	1.0 ± 0.14^{ab}	0.44 ± 0.07^{bcd}	0.77 ± 0.26^{abc}
F value	1.99*	2.41**	2.89**	2.88**

Values are presented as mean \pm standard deviation. Significant at $P < 0.001$. The values of identical letters within the same column are not significantly different based on Duncan's Multiple Range Test.

Large-scale cultivation, harvesting and drying

The biomass of T1 and T3 were harvested every 28 and 14 days, respectively, until the required quantities were obtained.



Photo 1. Large-scale cultivation of *C. vulgaris* using T1 and T3 treatments

PHB biopolymer extraction

The results of PHB extraction showed that its quantity in T3 has the highest value of $1364 \mu\text{g/g}$ followed by a value of $850 \mu\text{g/g}$ extracted from T1, as demonstrated in Fig. (1).

Characterization of the extracted PHB biopolymer by FTIR analysis

The FTIR spectra of PHB-T1 and PHB-T3 are presented in Fig. (3a, b), respectively, and are compared to the spectrum of commercial PHB, used as a standard, shown in Fig. (2). Both extracted samples exhibit characteristic absorption bands consistent with PHB functional groups.

A prominent absorption band is observed around 1029cm^{-1} , attributed to C–O stretching vibrations. A sharp peak at 1650cm^{-1} corresponds to C=O stretching, indicative of ester carbonyl groups. Additionally, a band is present between 1243 and 1155cm^{-1} , associated with C–O–C asymmetric stretching. A broader range of bands is evident between 1029 and 1457cm^{-1} , reflecting complex vibrational modes involving CH_2 bending and C–H stretching.

The absorption bands at 2925 and 2857cm^{-1} represent asymmetric and symmetric stretching vibrations of $-\text{CH}_2$ groups. Furthermore, a broad band near 3000cm^{-1} is observed, which may be associated with overlapping C–H stretches.

While the FTIR profiles of PHB-T1 and PHB-T3 closely resemble that of commercial PHB, minor spectral differences suggest slight structural variations, potentially due to impurities, residual biomass components, or differences in crystallinity of the extracted polymers from *C. vulgaris*.

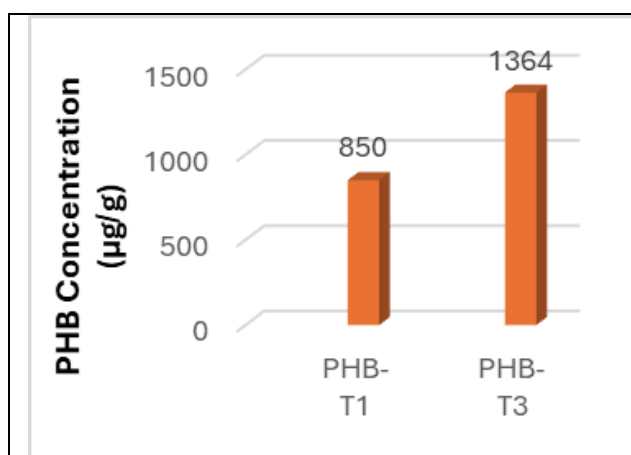


Fig. 1. PHB-T1 and PHB-T3 ($\mu\text{g/g}$) concentrations

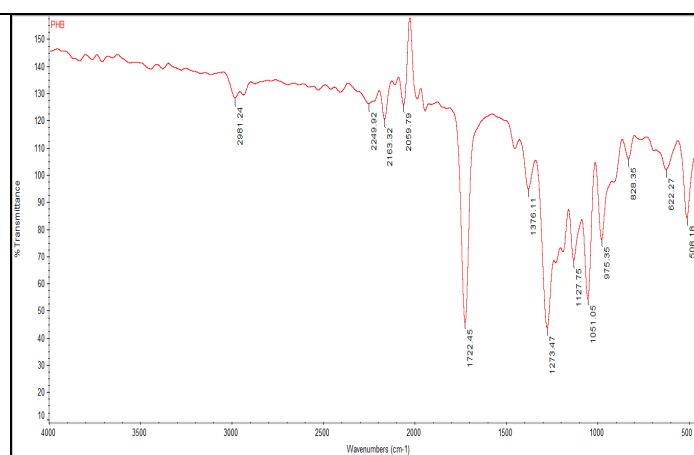


Fig. 2. FTIR spectra of commercial PHB

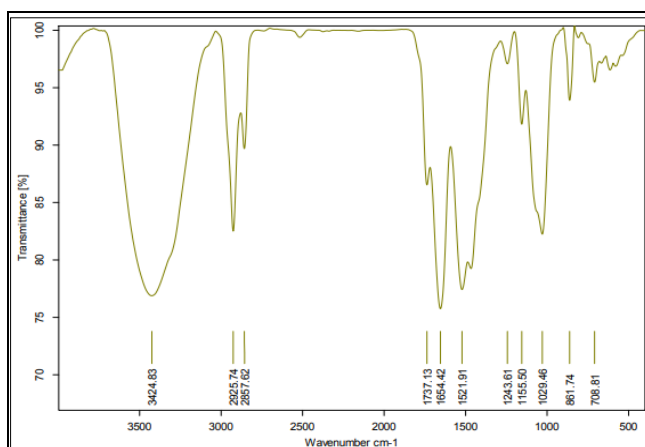


Fig. 3a. FTIR spectra for PHB-T1.

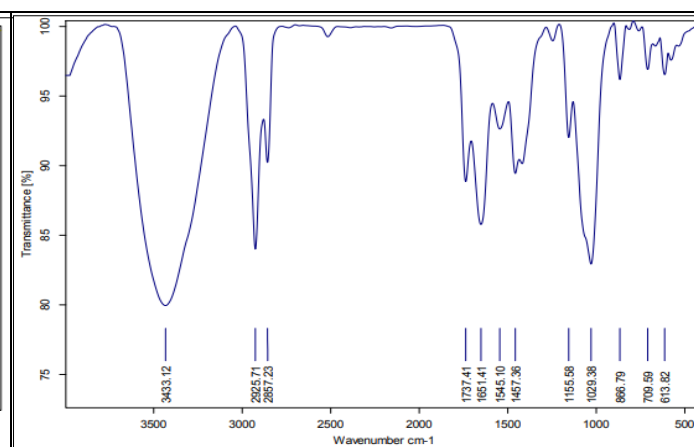


Fig. 3b. FTIR spectra for PHB-T3

Bioplastic formation from *C. vulgaris* and PHB

The results confirm that bioplastic films were successfully produced from dried *Chlorella vulgaris* biomass, as well as from PHB-T1 and PHB-T3 extracts. The characteristics of the resulting films are summarized below.




Bioplastic characterization

1. Physical properties

Color and texture

The visual evaluation of color and surface texture for all bioplastic films—those derived from dried *C. vulgaris*, PHB-T1, and PHB-T3—is presented in Table (3). These assessments were based on observable attributes such as surface uniformity, presence of cracks, film thickness, and color consistency.

Table 3. Color and texture properties of different bioplastic films

Picture			
Observation	The film is soft, free of cracks, thicker with a smooth surface and regular shape	The film is dry with cracks and thick. The surface is smooth and irregular shape	The film is dry with cracks and thick. The surface is smooth and irregular shape
Film	<i>C. vulgaris</i>	PHB-T1	PHB-T3

Solubility by solvent

The solubility of the bioplastic films in various solvents—acetone, ethanol, and chloroform—was evaluated at room temperature ($25 \pm 2^\circ\text{C}$) and 60°C after one hour of incubation. As shown in Fig. (4), significant differences in solubility were observed among the films and conditions ($P < 0.001$).

The *C. vulgaris*-based bioplastic film exhibited the highest solubility in both acetone and ethanol at 60°C , with values of $68.8 \pm 5.00\%$ and $59.5 \pm 0.50\%$, respectively. At room temperature, solubility values were slightly lower, recorded at $40.5 \pm 1.53\%$ for acetone and $53.3 \pm 0.50\%$ for ethanol. In contrast, the solubility in chloroform was consistently the lowest for the *C. vulgaris* film at both temperatures.

The PHB-T3 bioplastic film demonstrated moderate solubility, lower than the *C. vulgaris* film across all solvents, but slightly higher than that of PHB-T1, indicating intermediate solvent interaction properties. These results suggest that the bioplastic's

solubility behavior is strongly influenced by its composition, with *C. vulgaris*-based films showing greater solvent permeability, especially at elevated temperatures.

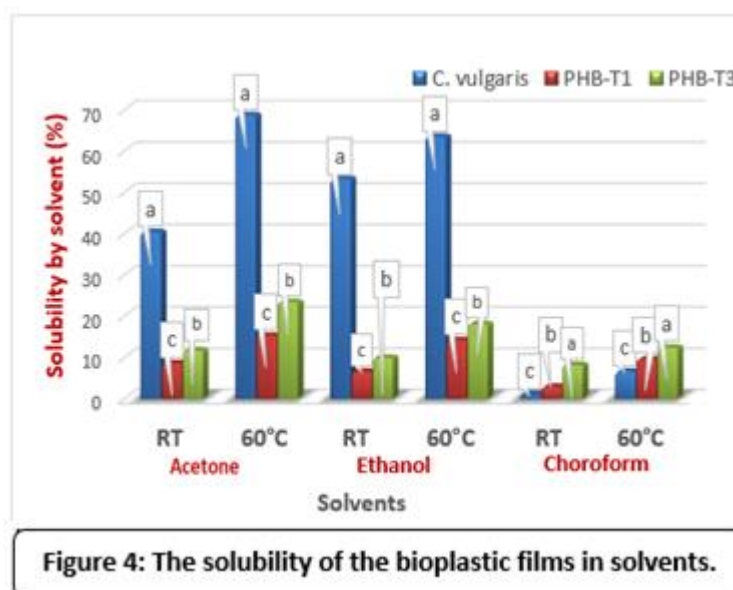


Figure 4: The solubility of the bioplastic films in solvents.

Moisture absorption

The moisture absorption capacity of the bioplastic films is presented in Fig. (5). The film made from *C. vulgaris* biomass exhibited the highest moisture absorption ratio, approximately 25%, which was significantly higher ($P < 0.05$) than those recorded for PHB-T1 and PHB-T3 films.

Among the PHB-based films, PHB-T1 showed the lowest moisture absorption, around 10%, while PHB-T3 demonstrated an intermediate absorption rate of approximately 15%. These results suggest that *C. vulgaris*-based films are more hydrophilic, likely due to the presence of residual algal components such as polysaccharides and proteins, which enhance water uptake compared to the more hydrophobic PHB films.

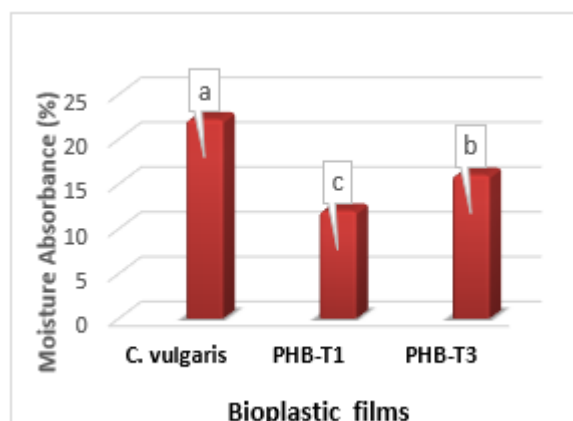


Figure 5: Moisture absorption of bioplastic films

Mechanical properties

The highest tensile strength (Fig. 6) was observed in *C. vulgaris* film at 9.5 MPa, while the lowest values recorded in PHB-T1 and PHB-T3 films were at 0.35 MPa. In contrast, the highest elongation break occurred in *C. vulgaris* film at 550% and the lowest value was in PHB-T3 film at 63%.

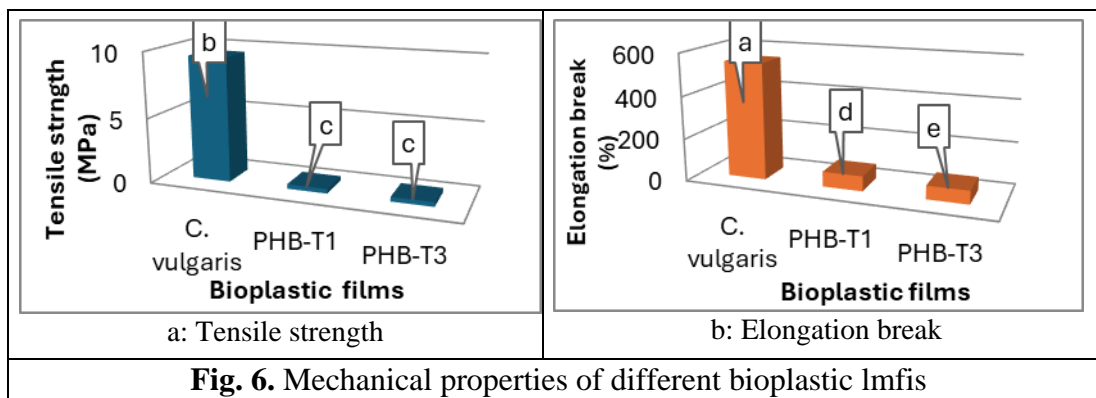


Fig. 6. Mechanical properties of different bioplastic films

Morphological properties: Scanning electron microscopy (SEM)

SEM images showed that the bioplastic *C. vulgaris* film had a surface with variations in distribution (Fig. 7a). Black spots or lumps distributed on the surface can be observed and the surface shows some roughness. The SEM image in Fig. (7b) shows that the bioplastic PHB-T1 film had a cracked and fissured surface compared to the previous sample. There are scattered white spots throughout the image, which may represent heterogeneous residues or impurities within the material. The surface appears rougher and has obvious cracks. Fig. (7c) shows that the surface of the bioplastic PHB-T3 film was irregular with scattered small cavities and pits.

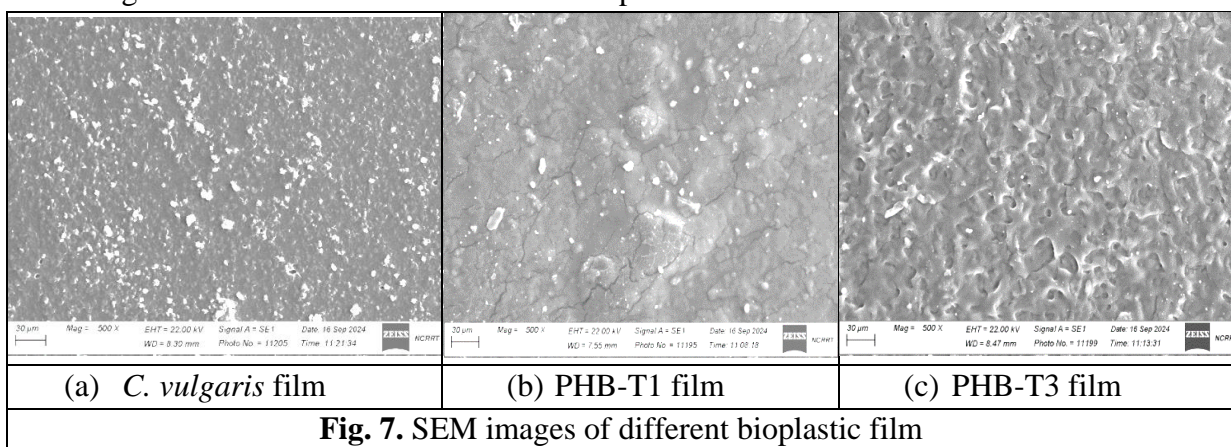


Fig. 7. SEM images of different bioplastic film

FTIR analysis

The data in Fig. (8) show peaks at 3283cm^{-1} , 2165 to 1935cm^{-1} . Additionally, the peaks were observed between 1624 and 1243cm^{-1} and between the ranges 1243 to 1037cm^{-1} . In Fig. (9a, b), the FTIR analysis of PHB-T1 and PHB-T3 films reveals several key peaks. The peaks were observed at 3280 and 3272cm^{-1} as well as 2927 and 2925cm^{-1} .

A peak was observed only in PHB-T1 at 1647cm^{-1} . There was a great similarity between both PHB-T1 and PHB-T3 films in FTIR analysis.

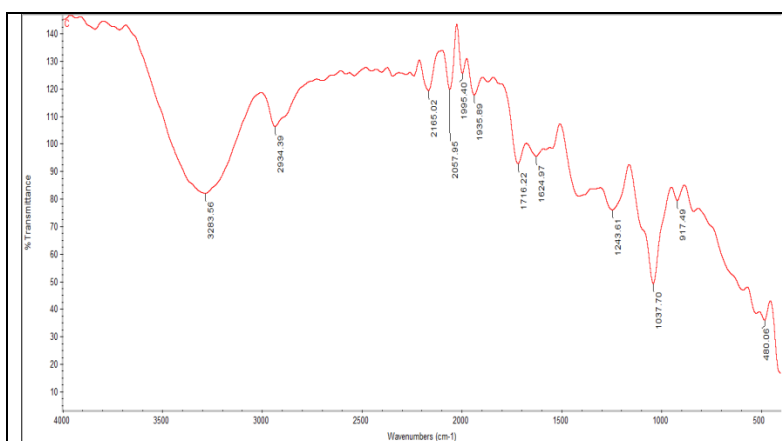


Fig. 8. FTIR spectra of bioplastic film obtained from *C. vulgaris*

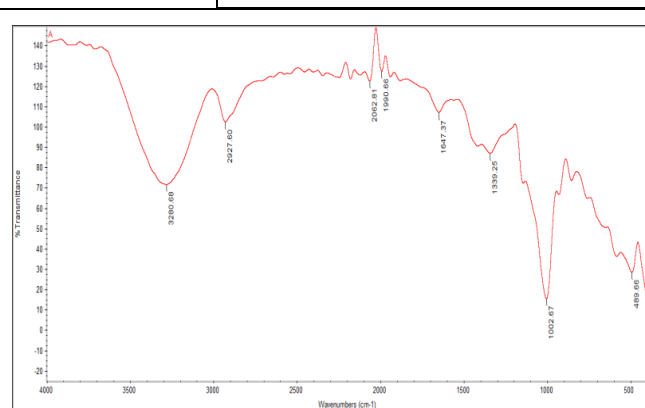


Fig. 9a. FTIR spectra of bioplastic film obtained from PHB-T1

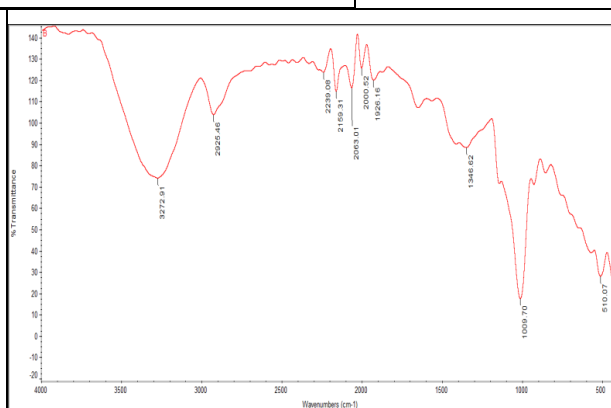


Fig. 9b. FTIR spectra of bioplastic film obtained from PHB-T3

XRD analysis

The XRD patterns for *C. vulgaris* bioplastic reveal strong reflections at 19.267° , 19.867° , 21.057° , and 22.300° , corresponding to intensities of 9615, 9137, 7858, and 5999, respectively, as shown in Fig. (10a). The XRD patterns of PHB-T1 and PHB-T3 samples were analyzed. Fig. (10b & c) shows the peaks in the XRD for PHB-T1 are approximately: 19.557° (9150), 21.649° (7447), 17.263° (5226), and 36.012° (1770). The peaks for PHB-T3 are approximately: 19.412° (5741), 21.278° (4350), 21.483° (3704), and 23.369° (2132).

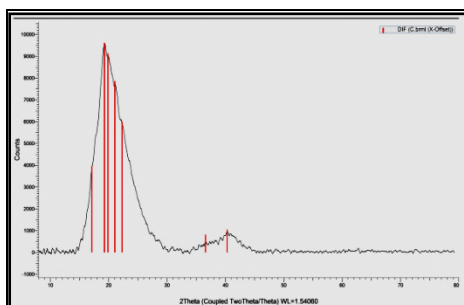


Fig. 10a. The XRD spectra of bioplastic obtained from *C. vulgaris*

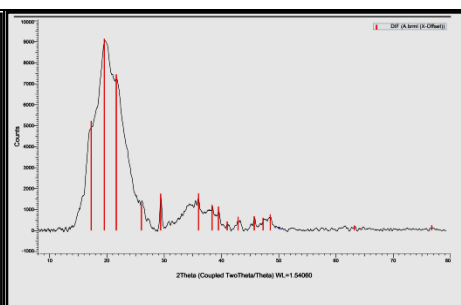


Fig. b. The XRD spectra of bioplastic film obtained from PHB-T1

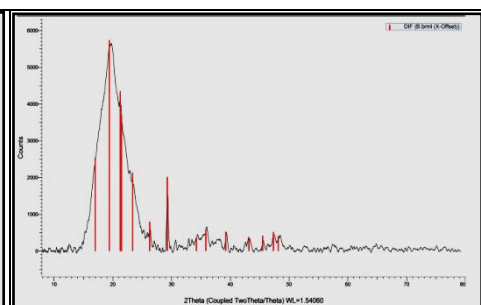
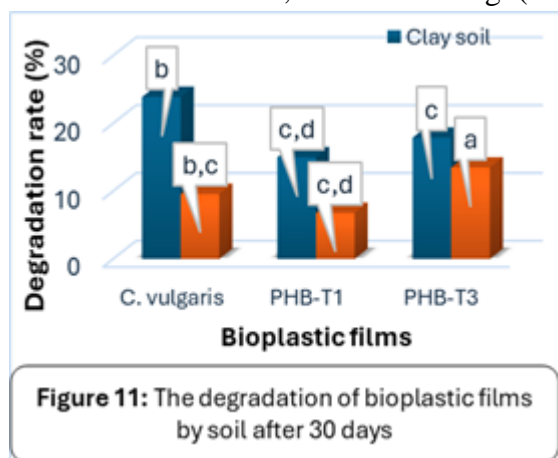


Fig. 10c. The XRD spectra of bioplastic film obtained from PHB-T3

Biological properties

* Biodegradation by soil

The results showed that all bioplastic films biodegraded more in clay soil than in sandy soil after films being buried for 30 days. In clay soil, the biodegradation rates were 23.9% for *C. vulgaris* film, 15.0% for PHB-T1 film and 17.9% for PHB-T3 film, while in sandy soil, the biodegradation rates were 9.6% for *C. vulgaris* film, 6.8% for PHB-T1 film and 13.5% for PHB-T3 film, as shown in Fig. (11).



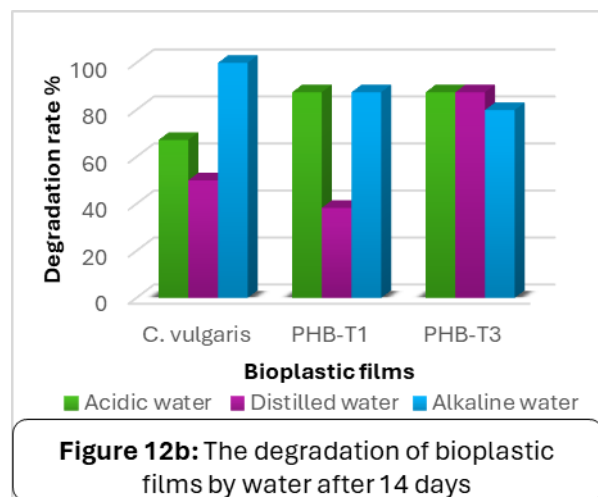
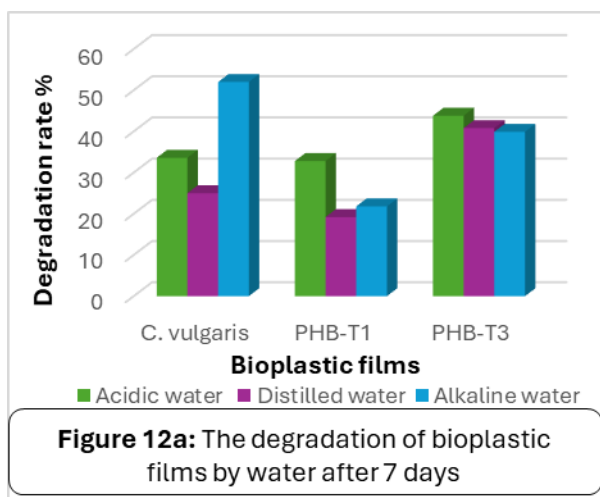
* Biodegradation by water

All bioplastic films were evaluated for solubility and biodegradation in acidic, distilled, and alkaline water over 7-day and 14-day intervals. Significant differences in solubility and degradation behavior were observed across the different media and film types ($P < 0.001$), as illustrated in Fig. (12a, b).

In acidic and distilled water, the PHB-T3 film exhibited the highest solubility, followed by the *C. vulgaris* film, with PHB-T1 showing the lowest solubility in both media. In alkaline water, this trend differed slightly—*C. vulgaris* film demonstrated the highest solubility, followed by PHB-T3, while PHB-T1 again recorded the lowest solubility.

After 14 days, biodegradation rates in acidic water reached 87.5% for both PHB-T1 and PHB-T3 films, which were higher than the *C. vulgaris* film (67.2%). In distilled water, PHB-T3 again showed the highest degradation (87.5%), followed by PHB-T1 (85.2%) and *C. vulgaris* (50%). However, in alkaline water, the degradation trend was reversed, with *C. vulgaris* film degrading the most, followed by PHB-T1, and the lowest degradation observed in PHB-T3.

These results demonstrate that the degradation and solubility behavior of the bioplastic films are strongly influenced by both the film composition and the chemical nature of the surrounding environment.



DISCUSSION

Modern life has been severely impacted by the rapid production and disposal of plastic waste. The accumulation of this waste in marine environments has been linked to numerous human health issues (Campanale *et al.*, 2020). Consequently, extensive research has been conducted on alternatives to these plastics, such as PHB, which serves as an excellent substitute for traditional petroleum-based plastics due to its similar properties to synthetic polymers and its biodegradability (Costa *et al.*, 2018; Silva & Houllou, 2022).

Most studies on various microalgae strains focus on modifying growth conditions to optimize PHB production (Pezzolesi *et al.*, 2023). The addition of sodium acetate to *C. vulgaris* media increased both growth and PHB production. This finding aligns with earlier research, which showed that supplementing phototrophic cultures with suitable organic carbon enhanced cellular productivity (Lowrey *et al.*, 2015). Similarly, Abdo and Ali (2019) reported that sodium acetate boosted PHB production in *Microcystis flosaquae*. Additionally, Heifetz *et al.* (2000) demonstrated that microalgal growth is influenced by carbon source concentration. These findings are supported by Li *et al.* (2020), who observed maximum cell counts with sodium acetate and higher light intensities. Studies also confirmed that acetate uptake and its conversion to acetyl-CoA enhance the acetyl-CoA pool, thereby stimulating the PHB pathway (Wu *et al.*, 2002;

Liu *et al.*, 2019). This was further verified when PHB levels increased by 81% in the presence of acetate compared to its absence (**Koch *et al.*, 2020**).

FTIR analysis of PHB-T1 and PHB-T3 (Figure 3; a & b) revealed spectra very similar to that of commercial PHB (Figure 2). Additional peaks at 1654 cm^{-1} and $1521\text{--}1527\text{ cm}^{-1}$, which were not observed in commercial PHB, indicate the presence of residual proteins or amide bonds. A distinct peak at 1647 cm^{-1} , found only in PHB-T1, suggests a weak C=O bond linked to conjugated carbonyl or amide groups. O–H stretching at 3242 cm^{-1} in PHB-T1 and PHB-T3—absent in commercial PHB—may point to structural modifications or incomplete/wet polymerization. FTIR results are consistent with those of **Kavitha *et al.* (2016)**, who identified absorption bands at 2933 cm^{-1} ($-\text{CH}_3$), 1728 cm^{-1} (C=O extension), and 1232 cm^{-1} (C–O–C stretching).

The solubility of these films indicates the presence of hydrophilic compounds, contributing to their classification as effective biodegradable materials (**Arham *et al.*, 2016**). In this study, PHB-T1 and PHB-T3 were more chemically stable. Acetone proved more effective than ethanol or chloroform as a solvent. The incorporation of PVA in the films may enhance the overall bioplastic properties (**El-Sheekh *et al.*, 2024**). Acetone's polar carbonyl and non-polar methyl groups enable interactions with both polar and non-polar substances, strengthening its solvent capacity.

Moisture content in bioplastic films reflects their ability to retain water vapor (**Singh *et al.*, 2014**). The *C. vulgaris* film absorbed more moisture, likely due to the algae's high hydroxyl and polar group content, which may limit its suitability for water-resistant applications. Conversely, PHB-T1 and PHB-T3 exhibited improved water resistance, potentially due to chemical changes during extraction or variations in polymer composition. **Nasir and Othman (2021)** found that increased glycerol content raised water content in bioplastics due to water–glycerol interaction. **Rahmadiawan *et al.* (2022)** further attributed moisture resistance to strong adhesion between algae and PVA, which reduces O–H groups and limits water diffusion.

The tensile strength of the *C. vulgaris* film was the highest ($\sim 9.5\text{ MPa}$), significantly outperforming PHB-T1 and PHB-T3 ($\sim 1\text{ MPa}$). This difference ($P < 0.05$) suggests that the structural composition of the algae film enhances molecular bonding and mechanical resistance. This improvement may stem from a higher concentration of polymeric components or a more uniform distribution in the film matrix. **Dianursanti *et al.* (2019)** explained that stronger PVA–algae adhesion results in a more homogeneous mix, increasing tensile strength. Likewise, **Ciapponi *et al.* (2019)** reported greater tensile strength with increased biomass concentration. Meanwhile, the lower strength in PHB-T1 and PHB-T3 may be due to voids or cracks formed during preparation. These results align with **Tsuji and Suzuyoshi (2002)**, who linked decreased tensile strength to cracks and pores in PHB films during biodegradation. Though PHB fibers are strong and elastic, their low elongation at break has been documented (**Kamravamanesh *et al.*, 2018**;

Saratale et al., 2020). In contrast, **Otsuki et al. (2004)** found that increasing biomass reduced both tensile strength and elongation.

Statistical analysis confirmed that the elongation at break differed significantly across the three films ($P < 0.05$). *C. vulgaris* exhibited the highest elongation (~550%), while PHB-T1 and PHB-T3 showed much lower values (~70% and ~50%, respectively), indicating reduced cohesion and greater brittleness. These results are consistent with **Abdo and Ali (2019)**, who found that microalgae-derived bioplastics had high elongation (~530%). According to **Amin et al. (2019)**, this may be due to increased polymer chain mobility, which enhances elasticity. The elongation of *C. vulgaris* films surpasses that of LDPE plastic (400%) and meets the UK ASTM D5336 standard (>500%). These results align with **Avérous (2008)** but exceed those reported by **Dianursanti et al. (2019)**.

SEM images at 500x magnification (Fig. 7a, b, and c) showed that PHB-T1 and PHB-T3 films had cracked, fissured surfaces with lumps, suggesting compositional changes or environmental effects on material integrity. According to **Gu and Wang (2013)**, such cracks may result from poor water retention by the polymer, causing rapid solvent evaporation and subsequent cracking. The white spots observed in SEM images, as noted by **Asif et al. (2021)**, likely indicate undissolved polymer particles or impurities caused by mechanical stress or partial biodegradation.

FTIR spectroscopy helps reveal chemical bonds and identify changes due to processing. It's widely used to detect key functional groups and molecular interactions in films (**Shen et al., 2021**). Figs. 8 and 9 (a & b) present FTIR spectra of bioplastics made from *C. vulgaris*, PHB-T1, and PHB-T3. All films displayed a peak at 3283 cm^{-1} , indicating free hydroxyl groups, consistent with findings by **Nešić et al. (2017)** and **Feng et al. (2022)**, and suggesting water solubility as noted by **Sabathini et al. (2018)**. A peak at 2934 cm^{-1} was associated with C—H bond stretching in polymer molecules (**Feng et al., 2022**). According to **Trakunjae et al. (2021)**, bands at 1716 cm^{-1} (in *C. vulgaris* only), 1243 cm^{-1} , and between $1000\text{--}1300\text{ cm}^{-1}$ correspond to C=O ester, —CH, and C—O groups, respectively. **Silva et al. (2020)** explained that the carbonyl peak at 1716 cm^{-1} in *C. vulgaris* may show slight shifts or reduced intensity due to water or impurities. The 1057 cm^{-1} peak corresponds to C—O and C=C bonds, while the $1600\text{--}1300\text{ cm}^{-1}$ range indicates the presence of amide groups and unbound proteins in *C. vulgaris* (**Reis et al., 2006**). Peaks between $1300\text{ \& }1000\text{ cm}^{-1}$ reflect C—O and C—O—C bonds from both PVA and *C. vulgaris*.

XRD analysis helps determine the chemical structure and degree of crystallinity, a key factor influencing a polymer's mechanical strength, brittleness, density, and transparency (**Shrivastava, 2018; Zhang et al., 2019; McAdam et al., 2020**). The XRD spectrum for *C. vulgaris* (Fig. 10) differed notably from those of PHB-T1 and PHB-T3. The *C. vulgaris* film showed broader and more prominent peaks than the typical

crystalline peaks at $2\theta = 19^\circ$ and 22° found in PHB, suggesting a more complex and varied structure due to the nature of algal biomass.

Biodegradation involves the breakdown of bioplastics into simpler organic compounds by microorganisms such as bacteria and fungi. In soil, these organisms secrete enzymes that degrade polymers into monomers, which are then metabolized into CO₂, water, and other byproducts (Adhikari *et al.*, 2016; Chamas *et al.*, 2020). The process starts with microbial colonization and biofilm formation on the plastic surface (Tosin *et al.*, 2019). Both bacterial and fungal communities—especially those in the Ascomycota phylum—play key roles in this degradation (Muroi *et al.*, 2016). Fungi physically interact with plastic surfaces, creating grooves and pits, often working in tandem with bacteria and actinomycetes.

Current findings showed that bioplastic films degraded faster in clay than sandy soil, with *C. vulgaris* films showing the highest degradation. This is supported by Singh *et al.* (2025), who attributed high biodegradability to the presence of carbon and oxygen functional groups. Clay soil, rich in nutrients, supports faster degradation through both microbial action and environmental factors (Kyrikou & Briassoulis, 2007). Additionally, Sudesh *et al.* (2000) highlighted that microbial depolymerases and various environmental variables drive PHB degradation.

The degradation of films exposed to different water types for 7 and 14 days (Fig. 12a, b) showed that *C. vulgaris* films were more soluble in alkaline water, while PHB films degraded more in acidic water. This may result from the strong attraction between glycerol and water molecules within the polymer matrix, allowing for rapid dissolution (Sanyang *et al.*, 2015). These findings align with Singh *et al.* (2025), who emphasized the variability in water-based degradation depending on glycerol levels. Other influencing factors include film morphology, the presence of free hydroxyl groups, and relative crystallinity. Li *et al.* (2018) noted that hydroxyl group interactions with water affect film hydrophilicity, while Sudheesh *et al.* (2020) stated that higher crystallinity reduces water penetration and degradability.

CONCLUSION

The production of polyhydroxybutyrate (PHB) from photosynthetic microorganisms represents a promising strategy for developing biodegradable plastic alternatives due to their cost-effectiveness and minimal environmental impact. Studies have shown that the addition of sodium acetate enhances PHB accumulation by increasing its intracellular concentration, which in turn promotes biofilm formation. The common alga *Chlorella vulgaris* has demonstrated great potential in the biosynthesis of biopolymers such as PHB. Furthermore, PHB production can be improved through specific nutrient supplementation strategies. Algal-based bioplastics, therefore, offer a sustainable and

environmentally friendly alternative to conventional plastics, with significant potential for industrial applications.

REFERENCES

- Abdo, S. M. and Ali, G. H. (2019):** Analysis of polyhydroxybutrate and bioplastic production from microalgae. *Bulletin of the National Research Centre*, 43(1), 1-4.
- Abou-El-Souod, G. W.; Hassan, L. H. and Morsy, E. M. (2016).** Comparison of different media formulations and the optimal growing conditions on growth, morphology and chlorophyll content of green alga, *chlorella vulgaris*. *Journal of American Science*, 12(6), 86-95.
- Adhikari, D.; Mukai, M.; Kubota, K.; Kai, T.; Kaneko, N.; Araki, K. S. and Kubo, M. (2016).** Degradation of bioplastics in soil and their degradation effects on environmental microorganisms. *Journal of Agricultural Chemistry and Environment*, 5(1), 23-34.
- Amin, M. R.; Chowdhury, M. A. and Kowser, M. A. (2019).** Characterization and performance analysis of composite bioplastics synthesized using titanium dioxide nanoparticles with corn starch. *Heliyon*, 5(8).
- Arham, R.; Mulyati, M. T.; Metusalach, M. and Salengke, S. (2016).** Physical and mechanical properties of agar based edible film with glycerol plasticizer. *International Food Research Journal*, 23(4).
- Arora, Y.; Sharma, S. and Sharma, V. (2023).** Microalgae in bioplastic production: a comprehensive review. *Arabian Journal for Science and Engineering*, 48(6), 7225-7241.
- Asif, M.; Tabassum, A.; Ali, T. M. and Rahman, A. (2021).** Preparation and estimation of physio-mechanical properties of eco-friendly bioplastics of *Gracilaria corticata* from Karachi coast. *Pak J Bot*, 53(4), 1525-1529.
- Avérous, L. (2008).** Polylactic acid: synthesis, properties and applications. In *Monomers, polymers and composites from renewable resources* (pp. 433-450). Elsevier.
- Campanale, C.; Massarelli, C.; Savino, I.; Locaputo, V. and Uricchio, V. F. (2020).** A detailed review study on potential effects of microplastics and additives of concern on human health. *International journal of environmental research and public health*, 17(4), 1212.
- Chamas, A.; Moon, H.; Zheng, J.; Qiu, Y.; Tabassum, T.; Jang, J. H., ... and Suh, S. (2020).** Degradation rates of plastics in the environment. *ACS Sustainable Chemistry & Engineering*, 8(9), 3494-3511.

- Chong, J. W. R.; Tan, X.; Khoo, K. S.; Ng, H. S.; Jonglertjunya, W.; Yew, G. Y. and Show, P. L. (2022).** Microalgae-based bioplastics: future solution towards mitigation of plastic wastes. *Environmental research*, 206, 112620.
- Ciapponi, R.; Turri, S. and Levi, M. (2019).** Mechanical reinforcement by microalgal biofiller in novel thermoplastic biocompounds from plasticized gluten. *Materials*, 12(9), 1476.
- Costa, S. S.; Miranda, A. L.; Andrade, B. B.; de Jesus Assis, D.; Souza, C. O.; de Moraes, M. G. ... and Druzian, J. I. (2018).** Influence of nitrogen on growth, biomass composition, production, and properties of polyhydroxyalkanoates (PHAs) by microalgae. *International journal of biological macromolecules*, 116, 552-562.
- Dang, B. T.; Bui, X. T.; Tran, D. P.; Ngo, H. H.; Nghiem, L. D.; Hoang, T. K. D. ... and Varjani, S. (2022).** Current application of algae derivatives for bioplastic production: A review. *Bioresource technology*, 347, 126698.
- Dianursanti; Noviasari, C.; Windiani, L. and Gozan, M. (2019, April).** Effect of compatibilizer addition in *Spirulina platensis*-based bioplastic production. In *AIP Conference Proceedings* (Vol. 2092, No. 1, p. 030012). AIP Publishing LLC.
- El-Sheekh, M. M.; Alwaleed, E. A.; Ibrahim, A. and Saber, H. (2024).** Preparation and characterization of bioplastic film from the green seaweed *Halimeda opuntia*. *International Journal of Biological Macromolecules*, 259, 129307.
- El-Sheekh, M.; Morsi, H. and Hassan, L. (2021).** Growth enhancement of *Spirulina platensis* through optimization of media and nitrogen sources. *Egyptian journal of Botany*, 61(1), 61-69.
- Feng, L.; Liu, H.; Li, L.; Wang, X.; Kitazawa, H. and Guo, Y. (2022).** Improving the property of a reproducible bioplastic film of glutenin and its application in retarding senescence of postharvest *Agaricus bisporus*. *Food Bioscience*, 48, 101796.
- Formela, K.; Kurańska, M. and Barczewski, M. (2022).** Recent advances in development of waste-based polymer materials: A review. *Polymers*, 14(5), 1050.
- García, G.; Sosa-Hernández, J. E.; Rodas-Zuluaga, L. I.; Castillo-Zacarias, C.; Iqbal, H. and Parra-Saldívar, R. (2020).** Accumulation of PHA in the microalgae *Scenedesmus sp.* under nutrient-deficient conditions. *Polymers*, 13(1), 131.
- Gu, L. and Wang, M. (2013).** Effects of protein interactions on properties and microstructure of zein–gliadin composite films. *Journal of Food Engineering*, 119(2), 288-298.

- Hassan, H.; Ansari, F. A.; Rawat, I. and Bux, F. (2024).** Drying strategies for maximizing polyhydroxybutyrate recovery from microalgae cultivated in a raceway pond: A comparative study. *Environmental Pollution*, 361, 124821.
- Heifetz, P. B.; Forster, B.; Osmond, C. B.; Giles, L. J. and Boynton, J. E. (2000).** Effects of acetate on facultative autotrophy in *Chlamydomonas reinhardtii* assessed by photosynthetic measurements and stable isotope analyses. *Plant Physiology*, 122(4), 1439-1446.
- Kamravamanesh, D.; Kovacs, T.; Pflügl, S.; Druzhinina, I.; Kroll, P.; Lackner, M. and Herwig, C. (2018).** Increased poly- β -hydroxybutyrate production from carbon dioxide in randomly mutated cells of cyanobacterial strain *Synechocystis sp.* PCC 6714: Mutant generation and characterization. *Bioresource technology*, 266, 34-44.
- Kaparapu, J. (2018).** Polyhydroxyalkanoate (PHA) production by genetically engineered microalgae: a review. *J. New Biol. Rep.*, 7(2), 68-73.
- Kartik, A.; Akhil, D.; Lakshmi, D.; Gopinath, K. P.; Arun, J.; Sivaramakrishnan, R. and Pugazhendhi, A. (2021).** A critical review on production of biopolymers from algae biomass and their applications. *Bioresource Technology*, 329, 124868..
- Kavitha, G.; Kurinjimalar, C.; Sivakumar, K.; Kaarthik, M.; Aravind, R.; Palani, P. and Rengasamy, R. (2016).** Optimization of polyhydroxybutyrate production utilizing waste water as nutrient source by *Botryococcus braunii* Kütz using response surface methodology. *International journal of biological macromolecules*, 93, 534-542.
- Koch, M.; Bruckmoser, J.; Scholl, J.; Hauf, W.; Rieger, B. and Forchhammer, K. (2020).** Maximizing PHB content in *Synechocystis sp.* PCC 6803: a new metabolic engineering strategy based on the regulator PirC. *Microbial cell factories*, 19, 1-12.
- Kyrikou, I. and Briassoulis, D. (2007).** Biodegradation of agricultural plastic films: a critical review. *Journal of Polymers and the Environment*, 15, 125-150.
- Li, L.; Chen, H.; Wang, M.; Lv, X.; Zhao, Y. and Xia, L. (2018).** Development and characterization of irradiated-corn-starch films. *Carbohydrate polymers*, 194, 395-400.
- Li, Y.; Huang, A.; Gu, W.; Wu, S.; Xie, X. and Wang, G. (2020).** Effects of inorganic carbon and light on acetate assimilation by *Nannochloropsis oceanica* (Eustigmatophyceae) in mixotrophic cultivation. *European Journal of Phycology*, 55(1), 64-75.

- Lichtenthaler, H. K. (1987).** Chlorophylls and carotenoids: pigments of photosynthetic biomembranes. In *Methods in enzymology* (Vol. 148, pp. 350-382). Academic Press.
- Liu, X.; Miao, R.; Lindberg, P. and Lindblad, P. (2019).** Modular engineering for efficient photosynthetic biosynthesis of 1-butanol from CO₂ in cyanobacteria. *Energy & Environmental Science*, 12(9), 2765-2777.
- Lowrey, J.; Brooks, M. S. and McGinn, P. J. (2015).** Heterotrophic and mixotrophic cultivation of microalgae for biodiesel production in agricultural wastewaters and associated challenges—a critical review. *Journal of applied phycology*, 27, 1485-1498.
- Madadi, R.; Maljaee, H.; Serafim, L. S. and Ventura, S. P. (2021).** Microalgae as contributors to produce biopolymers. *Marine Drugs*, 19(8), 466.
- Maheswari, N. U. and Ahilandeswari, K. (2011).** Production of bioplastic using *Spirulina platensis* and comparison with commercial plastic. *Res. Environ. Life Sci*, 4(3), 133-136.
- McAdam, B.; Brennan Fournet, M.; McDonald, P. and Mojicevic, M. (2020).** Production of polyhydroxybutyrate (PHB) and factors impacting its chemical and mechanical characteristics. *Polymers*, 12(12), 2908.
- Metzner, H.; Rau, H. and Senger, H. (1965).** Studies on synchronization of some pigment-deficient *Chlorella mutants*. *Planta*, 65, 186-194.
- Mohamed, H. E.; Abdo, S. M. and El Din, R. A. S. (2024).** Biopolymer detection in Egyptian microalgae: A pathway to eco-friendly bioplastics. *Bioresource Technology Reports*, 28, 102002.
- Muroi, F.; Tachibana, Y.; Kobayashi, Y.; Sakurai, T. and Kasuya, K. I. (2016).** Influences of poly (butylene adipate-co-terephthalate) on soil microbiota and plant growth. *Polymer Degradation and Stability*, 129, 338-346.
- Naesa, A.; Mona, R.; Kara-Ali, A. I. and Laika, H. E. (2019).** Economic and environmental side of the use of biotechnologies Case Study: Synthesis of some bioplastics from algae. *Studia Commercialia Bratislavensia*, 12(42).
- Nanda, N. and Bharadvaja, N. (2022).** Algal bioplastics: current market trends and technical aspects. *Clean Technologies and Environmental Policy*, 24(9), 2659-2679.
- Nasir, N. N. and Othman, S. A. (2021).** The Physical and Mechanical Properties of Corn-based Bioplastic Films with Different Starch and Glycerol Content. *Journal of Physical Science*, 32(3).

- Nešić, A.; Ružić, J.; Gordić, M.; Ostojić, S.; Micić, D. and Onjia, A. (2017). Pectin-polyvinylpyrrolidone films: A sustainable approach to the development of biobased packaging materials. *Composites Part B: Engineering*, 110, 56-61.
- Nguyen, D. M.; Do, T. V. V.; Grillet, A. C.; Thuc, H. H. and Thuc, C. N. H. (2016). Biodegradability of polymer film based on low density polyethylene and cassava starch. *International Biodeterioration & Biodegradation*, 115, 257-265.
- Onen Cinar, S.; Chong, Z. K.; Kucuker, M. A.; Wiecek, N.; Cengiz, U. and Kuchta, K. (2020). Bioplastic production from microalgae: a review. *International journal of environmental research and public health*, 17(11), 3842.
- Otsuki, T.; Zhang, F.; Kabeya, H. and Hirotsu, T. (2004). Synthesis and tensile properties of a novel composite of *Chlorella* and polyethylene. *Journal of applied polymer science*, 92(2), 812-816.
- Park, Y. K. and Lee, J. (2022). Achievements in the production of bioplastics from microalgae. *Phytochemistry Reviews*, 1-19.
- Pezzolesi, L.; Samorì, C.; Zoffoli, G.; Xamin, G.; Simonazzi, M. and Pistocchi, R. (2023). Semi-continuous production of polyhydroxybutyrate (PHB) in the Chlorophyta *Desmodesmus communis*. *Algal Research*, 74, 103196.
- Rahmadiawan, D.; Abral, H.; Railis, R. M.; Iby, I. C.; Mahardika, M.; Handayani, D. ... and Akbar, F. (2022). The enhanced moisture absorption and tensile strength of PVA/Uncaria gambir extract by boric acid as a highly moisture-resistant, anti-UV, and strong film for food packaging applications. *Journal of Composites Science*, 6(11), 337.
- Reis, E. F. D.; Campos, F. S.; Lage, A. P.; Leite, R. C.; Heneine, L. G.; Vasconcelos, W. L. ... and Mansur, H. S. (2006). Synthesis and characterization of poly (vinyl alcohol) hydrogels and hybrids for rMPB70 protein adsorption. *Materials Research*, 9, 185-191.
- Robert, R. and Iyer, P. R. (2018). Isolation and optimization of PHB (poly- β -hydroxybutyrate) based biodegradable plastics from *Chlorella vulgaris*. *Journal of Bioremediation & Biodegradation*, 2-5.
- Sabathini, H. A.; Windiani, L. and Gozan, M. (2018). Mechanical Physical properties of *Chlorella*-PVA based bioplastic with ultrasonic homogenizer. In *E3S Web of Conferences* (Vol. 67, p. 03046). EDP Sciences.
- Sanyang, M. L.; Sapuan, S. M.; Jawaid, M.; Ishak, M. R. and Sahari, J. (2015). Effect of plasticizer type and concentration on tensile, thermal and barrier properties

- of biodegradable films based on sugar palm (*Arenga pinnata*) starch. *Polymers*, 7(6), 1106-1124.
- Saratale, R. G.; Cho, S. K.; Ghodake, G. S.; Shin, H. S.; Saratale, G. D.; Park, Y., ... and Kim, D. S. (2020).** Utilization of noxious weed water hyacinth biomass as a potential feedstock for biopolymers production: A novel approach. *Polymers*, 12(8), 1704.
- Shen, Y.; Ni, Z. J.; Thakur, K.; Zhang, J. G.; Hu, F. and Wei, Z. J. (2021).** Preparation and characterization of clove essential oil loaded nanoemulsion and pickering emulsion activated pullulan-gelatin based edible film. *International Journal of Biological Macromolecules*, 181, 528-539.
- Shrivastava, A. (2018).** Plastic Properties and Testing. In *Plastics Design Library*; William Andrew Publishing: Norwich, NY, USA, 2018; pp. 49–110. [CrossRef]
- Silva, P. and Houllou, L. M. (2022).** Obtainment of Polyhydroxyalkanoates (PHAs) from Microalgae Supplemented with Agro-Industry Residue Corn Steep Liquor. *Journal of Botany Research*, 5(1), 138-140.
- Silva, V. D. M.; Macedo, M. C. C.; Rodrigues, C. G.; dos Santos, A. N.; e Loyola, A. C. D. F. and Fante, C. A. (2020).** Biodegradable edible films of ripe banana peel and starch enriched with extract of *Eriobotrya japonica* leaves. *Food bioscience*, 38, 100750.
- Singh, A. K.; Sharma, P.; Shrivastav, M.; Chaudhary, R.; Chauhan, P. and Banerjee, A. (2025).** PRODUCTION OF BIODEGRADABLE PLASTIC FILM FROM POTATO AND SAGO STARCH. *Journal of microbiology, biotechnology and food sciences*, e11143-e11143.
- Singh, P.; Nedumaran, S.; Ntare, B. R.; Boote, K. J.; Singh, N. P.; Srinivas, K. and Bantilan, M. C. S. (2014).** Potential benefits of drought and heat tolerance in groundnut for adaptation to climate change in India and West Africa. *Mitigation and adaptation strategies for global change*, 19, 509-529.
- SPSS, I. (2012).** SPSS version 16.0 User's guide. SPSS inc., Chicago, USA
- Stanier, R. Y.; Kunisawa, R.; Mandel, M. C. B. G. and Cohen-Bazire, G. (1971).** Purification and properties of unicellular blue-green algae (order Chroococcales). *Bacteriological reviews*, 35(2), 171-205.
- Sudesh, K.; Abe, H. and Doi, Y. (2000).** Synthesis, structure and properties of polyhydroxyalkanoates: biological polyesters. *Progress in polymer science*, 25(10), 1503-1555.

- Sudheesh, C.; Sunooj, K. V.; Sasidharan, A.; Sabu, S.; Basheer, A.; Navaf, M., ... and George, J. (2020).** Energetic neutral N₂ atoms treatment on the kithul (*Caryota urens*) starch biodegradable film: Physico-chemical characterization. *Food Hydrocolloids*, 103, 105650.
- Tosin, M.; Pischedda, A. and Degli-Innocenti, F. (2019).** Biodegradation kinetics in soil of a multi-constituent biodegradable plastic. *Polymer Degradation and Stability*, 166, 213-218.
- Trakunjae, C.; Boondaeng, A.; Apiwatanapiwat, W.; Kosugi, A.; Arai, T.; Sudesh, K. and Vaithanomsat, P. (2021).** Enhanced polyhydroxybutyrate (PHB) production by newly isolated rare actinomycetes *Rhodococcus* sp. strain BSRT1-1 using response surface methodology. *Scientific reports*, 11(1), 1896.
- Tsuji, H. and Suzuyoshi, K. (2002).** Environmental degradation of biodegradable polyesters 1. Poly (ϵ -caprolactone), poly [R]-3-hydroxybutyrate], and poly (L-lactide) films in controlled static seawater. *Polymer Degradation and Stability*, 75(2), 347-355.
- Tun, T. Y. and Mar, A. A. (2020).** *Preparation and characterization of starch-based bioplastic film from dent corn* (Doctoral dissertation, MERAL Portal).
- Wu, G.; Bao, T.; Shen, Z. and Wu, Q. (2002).** Sodium acetate stimulates PHB biosynthesis in *Synechocystis* sp. PCC 6803. *Tsinghua Science and Technology*, 7(4), 435-438.
- Wu, Y.; Geng, F.; Chang, P.R.; Yu, J. and Ma, X. (2009).** Effect of agar on the microstructure and performance of potato starch film. *Carbohydrate Polymers*, 76(2), pp. 299-304.
- Zainan, N. H.; Srivatsa, S. C.; Li, F. and Bhattacharya, S. (2018).** Quality of bio-oil from catalytic pyrolysis of microalgae *Chlorella vulgaris*. *Fuel*, 223, 12-19.
- Zhang, C.; Show, P. L. and Ho, S. H. (2019).** Progress and perspective on algal plastics—a critical review. *Bioresource technology*, 289, 121700.